Effect of Water on Overbased Sulfonate Engine Oil Additives

J. W. Tavacoli,[†] P. J. Dowding,[‡] D. C. Steytler,[§] D. J. Barnes,[||] and A. F. Routh*,[⊥]

Department of Chemical and Process Engineering, University of Sheffield, Mappin Street, Sheffield S1 3JD, United Kingdom, Infineum UK Limited, Milton Hill, Abingdon, Oxfordshire OX1 36BB, United Kingdom, School of Chemical Sciences & Pharmacy, University of East Anglia, Norwich NR4 7TJ, United Kingdom, LGC, The Heath, Runcorn, Cheshire WA7 4QX, United Kingdom, and Department of Chemical Engineering, University of Cambridge, BP Institute, Madingley Road, Cambridge CB3 0EZ, United Kingdom

Received November 26, 2007. In Final Form: January 16, 2008

The presence and effect of water on calcium carbonate nanoparticles used in engine additives, stabilized with a sulfonate surfactant, is investigated using small-angle neutron scattering, dynamic light scattering, Fourier transform infrared spectroscopy, and rheometry. These techniques provide complementary data that suggests the formation of a layer of water around the core of the particles ensuring continued colloidal stability yet increasing the dispersion viscosity. Through the use of small-angle neutron scattering, the dimensions of this layer have been quantified to effectively one or two water molecules in thickness. The lack of a significant electrostatic repulsion is evidence that the water layer is insufficient to cause major dissociation of surface ions.

Introduction

An overbased sulfonate engine oil additive (OBSA) consists of a core of amorphous calcium carbonate surrounded by a monolayer of alkyl aryl sulfonate surfactant. The core is generally less than 10 nm in diameter.

The stability of such dispersions is crucial for their correct performance, and the surfactant provides steric stabilization preventing coagulation. There is anecdotal evidence that water plays a role in the destabilization of overbased engine oil additives, and because the combustion process can produce a considerable amount of water, the effect on calcium carbonate particles requires investigation.

Whereas the effect of electrostatic potentials in organic media is usually ignored, there is a growing literature demonstrating long-range repulsion between some particles.[1] If water is present in these systems, either at the particle surfaces or as microemulsions, then it is possible to envisage a situation where charge dissociation could occur, and this could lead to an electrostatic potential.

OBSA additives are synthesized in a one-pot process in which CO_2 is blown through a mixture originally containing aqueous $Ca(OH)_2$, alkyl aryl sulfonic acid surfactant, and apolar solvents,[2] with the effect of converting the hydroxide into carbonate. It has been stipulated that this process takes place via a w/o microemulsion, and hence a sub-50-nm particle size is achieved.[2,3] OBSA particles are included in lubricant formulations to provide acid neutralization (arising from the oxidation of the base fluid and acidic "blow-by" gases originating from the combustion of fuel) and piston cleanliness. A measure of the acid neutralization potential of OBSA particles is given by the total base number (TBN). This is simply the amount of KOH in milligrams that is equivalent to 1 g of OBSA material with respect to acid titration, and hence TBN has units of mg KOH/g. Inorganic acid transfer may occur across the water−oil interface of macroscopic water droplets/films, but an alternative mechanism is considered to take place through base transfer from the OBSA particles to acidic microemulsion droplets on Brownian collision.[4,5] The presence of water has been shown to have a detrimental effect on the efficiency of OBSA-facilitated acid neutralization,[6] and as such, the understanding of water−OBSA interactions is of great importance. In this article, we monitor interactions through dynamic light scattering (DLS), Fourier transform infrared spectroscopy (FTIR), small-angle neutron scattering (SANS), and rheometry. A schematic of an OBSA particle similar to those used in this study is shown in Figure 1.

Whereas the presence of water in engine oils is well known, the location of the water molecules has not been elucidated before. Conceptually, there are three locations that water can occupy in such a system: (1) water-in-oil microemulsions could form, presumably stabilized by free surfactant, (2) water could penetrate throughout the calcium carbonate particles, or (3) water can be located at the surface of particles. In this article, we will present evidence from a number of techniques that the water is located at the particle surface. The particles remain hard-sphere-like, negating the possibility of electrostatic repulsion, and there is evidence from SANS experiments that microemulsions are not forming.

Experimental Section

Materials. The overbased 300 TBN calcium sulfonate engine oil additive (OBSA) (55 wt % in base oil) was provided by Infineum UK Limited. Anhydrous-grade dodecane and cyclohexane, anhydrous calcium chloride, molecular sieves (3 Å), and deuterated water were all purchased from Sigma-Aldrich and used as received.

Dynamic Light Scattering Experiments. The supplied OBSA particles were diluted to 3.3 wt % solids in dodecane. The solution

* Corresponding author. E-mail: afr10@cam.ac.uk. Tel: +44 1223 765718. Fax: +44 1223 765701.
[†] University of Sheffield.
[‡] Infineum UK Limited.
[§] University of East Anglia.
[||] LGC.
[⊥] University of Cambridge.

(1) Hsu, M. F.; Dufresne, E. R.; Weitz, D. A. *Langmuir* **2005**, *21*, 4881−4887.
(2) Galsworthy, J.; Hammond, S.; Hone, D. *Curr. Opin. Colloid Interface Sci.* **2000**, 274−2790.
(3) Roman, J.-P., et al. *J. Colloid Interface Sci.* **1991**, *144*, 324−339.
(4) Hone, D. C., et al. *Can. J. Chem.* **1999**, *77*, 842−848.
(5) Hone, D. C.; Robinson, B. H.; Steytler, D. C. *Langmuir* **2000**, *16*, 340−346.
(6) Fox, M. F.; Picken, J. D.; Pawlak, Z. *Tribol. Int.* **1990**, *23*, 183−185.

10.1021/la703680e CCC: $40.75
Published on Web 02/27/2008

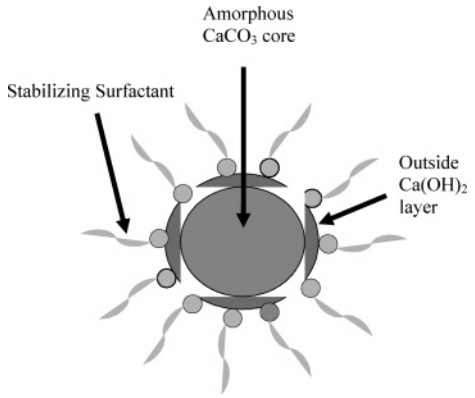

Figure 1. Schematic of the structure of an overbased additive particle.

was then filtered (poly(tetrafluoroethylene) (PTFE), 0.2 μm), dried with $CaCl_2$, and split into two fractions. One fraction was placed in a vacuum desiccator containing silica gel, and the other, in a vacuum desiccator containing an open beaker of water. These desiccators correspond to dry and water-saturated environments. The desiccators were vacuum sealed and reopened only to take samples for light scattering measurements. These took place over 65 days using a Brookhaven ZetaPals fitted with a 50 mW laser of wavelength 632 nm.

FTIR Experiments. The OBSA mineral oil solution was diluted to a particle concentration of 25 wt % and then placed in a water-saturated desiccator. FTIR spectra were collected over a period of 16 weeks using a Perkin-Elmer Spectrum One FTIR spectrometer with a resolution of 0.5 cm^{-1}. To obtain the spectra, the samples were loaded into a BaF_2 flow cell with a fixed path length of 0.5 mm.

SANS Experiments. SANS data were collected from the National Institute of Standards and Technology (NIST) based in Washington D.C. using the NG7 SANS instrument. A 3.9 wt % additive dilution was made in cyclohexane. This dispersion was dried using molecular sieves (predried overnight in a conventional oven at 200 °C) and filtered (0.2 μm, PTFE). From this, an aliquot was taken to which D_2O (15 wt %) was added. This mixture was gently shaken to ensure D_2O saturation, after which the formation of two transparent and distinct phases of oil and water quickly followed. Aliquots of the original and D_2O-saturated additive solutions were then taken and transferred to quartz cells with path lengths of 1 mm. Additionally, a 3.2 wt % OBSA dispersion in D-cyclohexane, dried in the same manner as above, was used to measure the surfactant layer length. In these experiments, cells with a path length of either 2 or 5 mm were used. In the SANS setup, the detector distance and offset angle were 2 m and 20°, respectively, the incident wavelength was 8 Å, and the effective Q range extended from 0.01 to 0.21 $Å^{-1}$.

SANS Theory. The normalized scattering intensity arising from the SANS analysis of a monodisperse system containing spherical particles may be written as[7,8]

$$I(Q) = n_P P(Q)\, S(Q) \tag{1}$$

where n_P is the particle number density, Q is the scattering vector, $S(Q)$ is the structure factor, and $P(Q)$ is the form factor that, for a core−shell system as shown in Figure 2, is[9]

$$P(Q) = \left\{ \begin{aligned} &(\rho_A - \rho_M)\left(V_T \frac{3(\sin(QR_T) - QR_T\cos(QR_T))}{(QR_T)^3} - \right. \\ &\left. V_P \frac{3(\sin(QR_P) - QR_P\cos(QR_P))}{(QR_P)^3} \right) \\ &+ (\rho_P - \rho_M) V_P \frac{3(\sin(QR_P) - QR_T\cos(QR_P))}{(QR_P)^3} \end{aligned} \right\}^2 \tag{2}$$

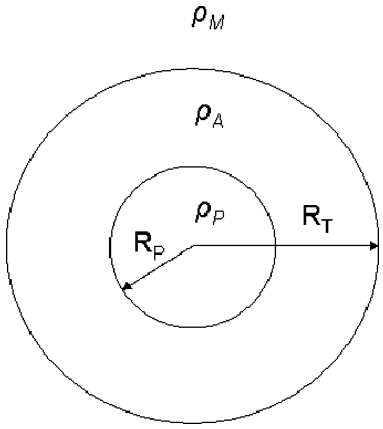

Figure 2. Schematic showing how a core−shell particle is represented in the SANS analysis.

Here, ρ is the scattering length density (SLD) and subscripts A, P, and M refer to the absorbed layer, the particle core, and the dispersing medium, respectively. V_P is the volume of the core, and V_T is the total volume of the spherical core−shell particle. If the SLDs of the absorbed layer and the medium are matched (i.e., $\rho_A = \rho_M$), then eq 2 becomes

$$P(Q) = \left((\rho_P - \rho_M) V_p \frac{(3\sin(QR_P) - QR_P\cos(QR_P))}{(QR_P)^3} \right)^2 \tag{3}$$

which is the form factor of a homogeneous particle.

Additionally, a Schultz distribution,[11] $X(R_i)$, may be used to model the effect of a dispersion's polydispersity on the intensity of scattering as follows

$$I(Q) = \phi_p \left[\sum_i^{R_{max}} P(Q, R_i)\, X_i(R_i) \right] S(Q) \tag{4}$$

where the distribution, normalized using the core volume fraction, ϕ_p, extends to a maximum radius, R_{max}. A Schultz distribution takes the form of a Gaussian skewed to larger sizes.

To account for hard-sphere particle interactions, the $S(Q)$ term takes the form as described by Aschroft and Leckner.[10]

Rheometry Experiments. OBSA dispersions of approximately 28, 30, 33, 36, 39, and 44 wt % were made in dodecane, after which any water contamination was removed with the addition of a predried molecular sieve. All dilutions were then split into two portions, and excess water (15 wt %) was added to one portion. These wet samples were then gently shaken to ensure water saturation. After the formation of two distinct regions of water and oil, the viscosities of the wet and dry samples were ascertained using a Bohlin CVO rheometer attached with Mooney Ewart geometry. For the measurements, a stress ramp proceeding from 1 to 6 Pa was applied. For measurement calibration, the viscosity of dodecane and base oil mixtures correlating to the dilutions above were also measured. Additionally, the wet and dry viscosities of the dodecane and base oil solvents were measured, and no difference was found between the two states. In Figure 3, the viscosity of a 62 wt % solution of a wet sample is plotted as a function of measurement time. A considerable reduction in viscosity is noticed in the early portion of the measurement, and the reported viscosity value is taken from where the viscosity remained constant. In all samples, this was when the shear stress was held at 6 Pa, the region from 60 s onward in Figure 3.

Results

DLS. The results of the DLS measurements are shown in Figure 4, and it is evident that both the wet and dry fractions of

(7) Eastoe, J. *Scattering Techniques*; http://www.chm.bris.ac.uk/pt/eastoe/chapters%20oct%202003/4%20Scattering%20techniques.pdf. University of Bristol, 2003.

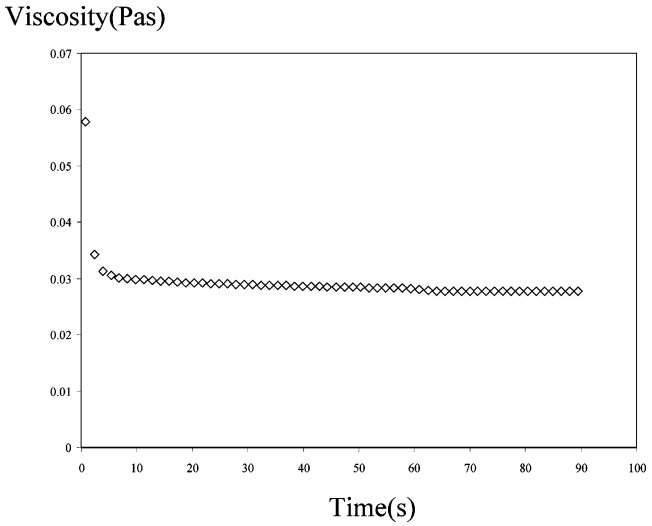

Figure 3. Measured viscosity of a 62 wt % wet sample in dodecane from start up.

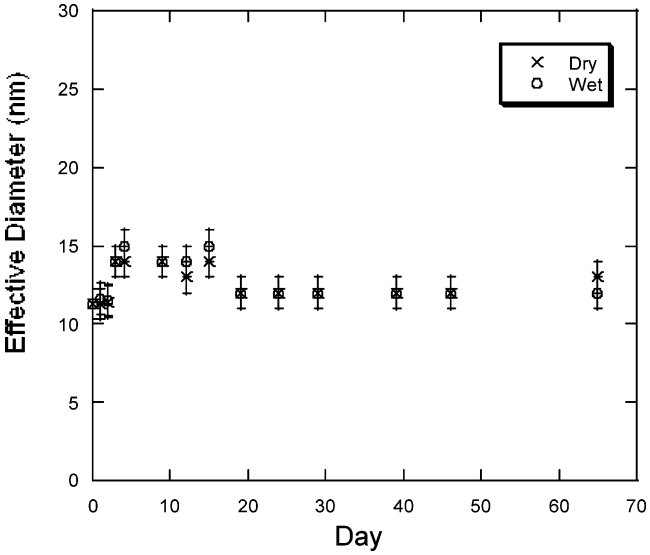

Figure 4. Size of identical additive dilutions stored in dry (×) and wet (○) environments, as measured by dynamic light scattering.

the additive remain stable with an absence of attractive interactions over 70 days with the hydrodynamic diameters remaining at about 12 nm.

FTIR. The labeled IR spectra of the OBSA dodecane solution with different exposures to the water-saturated environment are shown in Figure 5. The aliphatic peaks (∼1300−1600 cm^{-1}) result from the base oil, dodecane, and the additive's steric stabilizing surfactant chains. The broad calcium carbonate peak, which originates from the particles, appears in the range of 1300−1600 cm^{-1}. As expected, with increased exposure of the OBSA dodecane solution to the water-saturated environment, water is taken up, which is evident through increased absorption in the hydroxyl stretching region of 3650−3100 cm^{-1} and in the water banding peak at 1640 cm^{-1}. On closer inspection and as demonstrated in Figure 6, two water peaks exist at around 3450 and 3190 cm^{-1}. Though both peaks show increased absorbance during the experiment, the size of the peak at 3450 cm^{-1} becomes increasingly larger than the lower water peak such that toward the end of the experiment it is hard to distinguish the peak at 3190 cm^{-1}.

The IR peaks associated with the sulfonate group are found in the 1200−1000 cm^{-1} region, and they shift to lower energies as the experiment progresses. This can be observed more clearly in Figures 7 and 8, which show the peak maxima for the asymmetric and symmetric vibrations, respectively. Because the experiment duration is coupled with increased water absorption, it is apparent that these peak shifts are a result of additive facilitated water uptake and specifically water−sulfonate surfactant interactions.

SANS. All of the scattering data was normalized against cell and solvent scatter and converted to absolute intensities using a polymer standard.

The data was fitted using the FISH program, written and developed by Richard Heenan (ISIS, U.K.), and fit iteration proceeded via a 64-point Gaussian quadrature method. The SLD values, which were used in this investigation, are displayed in Table 1.

Figure 9 shows the scattering resulting from the dry and D_2O-doped OBSA dispersions. The intensity of the D_2O-doped dispersion is significantly greater at low Q in comparison to that of the undoped dispersion. Because the uptake of water by ABS in the form of w/o microemulsions is known to be low, the scattering obtained in the presence of added water is strongly suggestive of hydration of the particle core. An increase in intensity (as is given) would result through contrast contribution to the scattering if the water simply hydrated the core without increasing its size. However, the shape of the scattering also indicates an increase in size of the core, which suggests that the water is adsorbed as a surface layer.

This structure was elucidated as follows: First the scattering derived from the dry sample was fitted using a Schultz polydisperse model (with R_{max} set to 6 nm) undergoing hard-sphere interactions. In this manner, the core radius was ascertained because the SLD of the surfactant layer can be approximated to be the same as that of the cyclohexane solvent. Because the concentration of the Infineum OBSA base oil dilution is not accurately known, the fitting took place by floating the particle volume fraction within estimated limits in addition to the polydispersity, $S(Q)$ (as a hard-sphere volume fraction), hard-sphere radius, and core radius though these last three fitting parameters were held after the first fit (and some experimenting) to simplify the procedure. The constant fitting parameter was then the SLD of calcium carbonate, which was adjusted to accommodate a density range of 2−2.8 g cm^{-3}.

Subsequently, the fitted values obtained from the core fits were used to parametrize a Schultz polydisperse core−shell model used to fit the data produced from the D_2O-doped OBSA dodecane dilution. Hence, in these fits, the only floated parameter was the length of an absorbed layer of D_2O. Using this combination of core and core shell fits, a core radius of 2.79 nm and a surrounding D_2O layer of 0.39−0.54 nm, depending on the calcium carbonate density, were calculated. Fit quality varied only slightly with changes in calcium carbonate density, and fit details are presented in Table 2. In Figure 9, core and core−shell fits using a calcium carbonate density of 2.0 g cm^{-3} can be seen, and it is apparent that the core−shell model replicates the data very well, providing evidence for a shell of D_2O forming around the OBSA's calcium carbonate core, probably corresponding to a multilayer of molecules.

The parameters used in the core fits were also used in the surfactant layer length fits. The hard-sphere and particle volume fractions were scaled down accordingly with relation to the

(8) Ottewill, R. H. *Small Angle Neutron Scattering in Colloidal Dispersions*; 1982, pp 143−163.
(9) Markovic, I.; Ottewill, R. H. *Colloid Polym. Sci.* **1986**, *264*, 65−76.
(10) Ashcroft, N. W.; Lekner, J. *Phys. Rev.* **1966**, *145*, 83−90.
(11) Kotlarchyk, M.; Chen, S.-H. *J. Chem. Phys.* **1983**, *79*, 2461−2469.

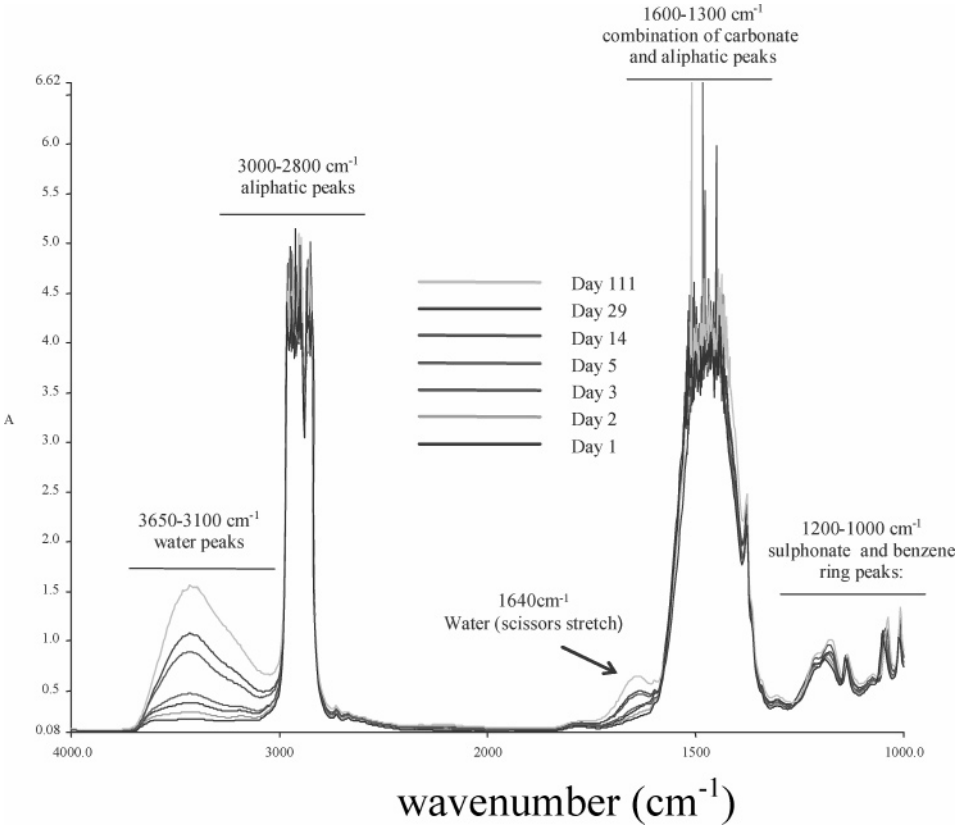

Figure 5. FTIR spectrum of an OBSA dilution in dodecane with varied durations in a water-saturated environment.

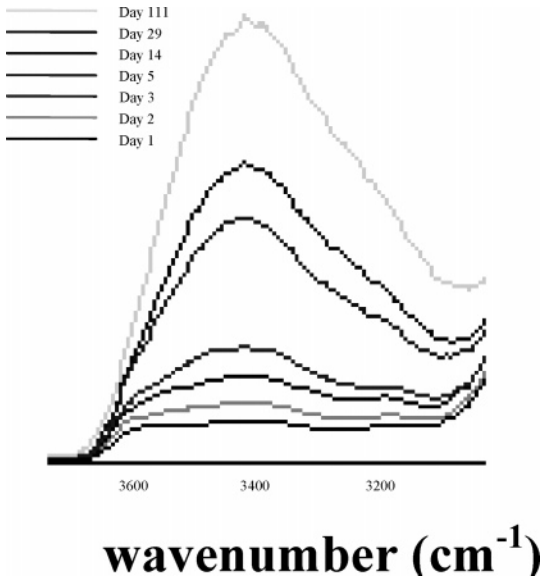

Figure 6. Change in the water-related FTIR peaks of the additive with increasing exposure to a water-saturated environment.

dispersion concentrations in H-cyclohexane and D-cyclohexane, and again the SLD of H-cyclohexane was used to represent the surfactant layer. Fit details may be seen in Table 3, and one can see that the layer length varies significantly with calcium carbonate density, ranging from 1.42 nm at a density of 2.0 g cm^{-3} to 2.02 nm at 2.8 g cm^{-3}. The best fits occur at densities of 2.2 and 2.4 g cm^{-3} with corresponding surfactant layer lengths of 1.62 and 1.76 nm, respectively. A total diameter of around 9 nm then seems likely, which is in reasonable accordance with the DLS-measured diameters. A surfactant layer length fit is displayed in Figure 10, and the details of the fits may be seen in Table 3.

As a control to the D_2O-doped OBSA disperions, SANS measurements were made on a D_2O-doped sulfonate surfactant solution at a higher concentration of active material (i.e., there was more surfactant material here than there was both surfactant and base combined in the OBSA solution). Some, but importantly less, scattering was observed in this case. From this we may conclude that the increased intensity apparent in the D_2O-doped OBSA solution over its dry analogue, even in the worst case (and unrealistic) scenario of all the surfactant material being unattached from the calcium carbonate core, must at least partially originate from D_2O present at the surface of the particle. The formation of even small numbers of microemulsion droplets in the OBSA solution would produce some of the additional scattering, but this cannot explain the observed scattering intensity that can only be due to a D_2O structure on the same size scale as that of the particles. Hence, we are observing a water layer of about 0.5 nm thickness.

Rheometry. Figure 11 shows a plot of viscosity versus volume fraction for the wet and dry samples of the OBSA dodecane dilutions. What is clear is that the wet samples have a higher viscosity than the dry samples and with an increase in volume fraction the viscosity jump in the wet samples becomes greater.

The hard-sphere volume fraction values were calculated by scaling up from the best fit volume fraction provided by the surfactant layer length fits. The volume fractions shown in Figure 11 are calculated using an R_{HS} of 4.5 nm, but as will be discussed later, the extent to which the volume fraction values of the wet samples must be adjusted such that both sets of data fit on a master curve is quite insensitive to the volume fraction range.

For the data shown in Figure 12, increasing the value of the particle diameter for the wet sample by 0.05 nm shifts the volume fraction values and collapses all of the data points to a single

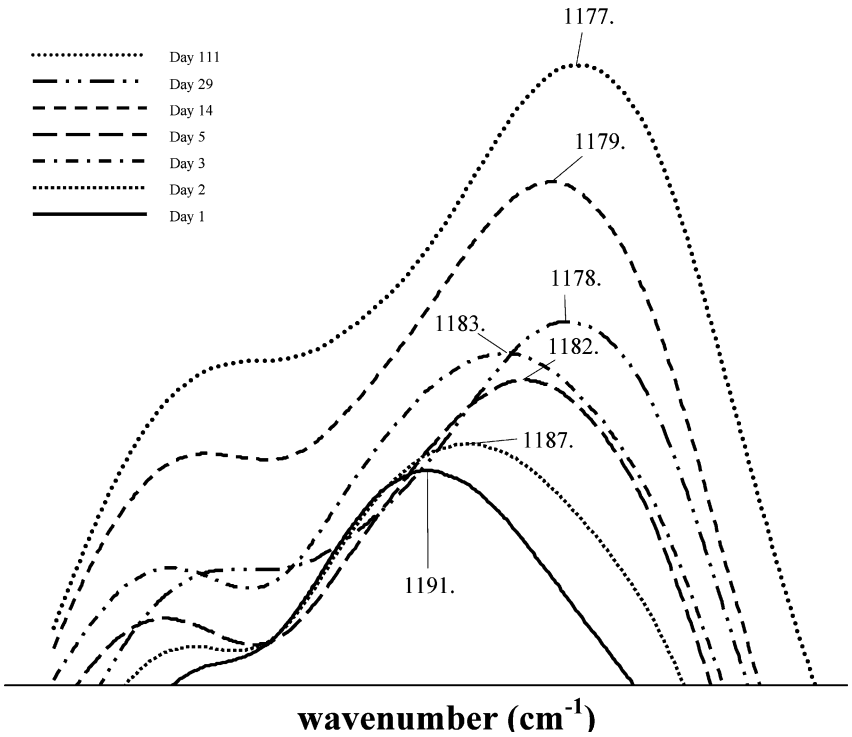

Figure 7. Expanded IR region of the asymmetric sulfonate peak showing the shifting of the peak to lower wavenumbers with increasing exposure to a water-saturated environment.

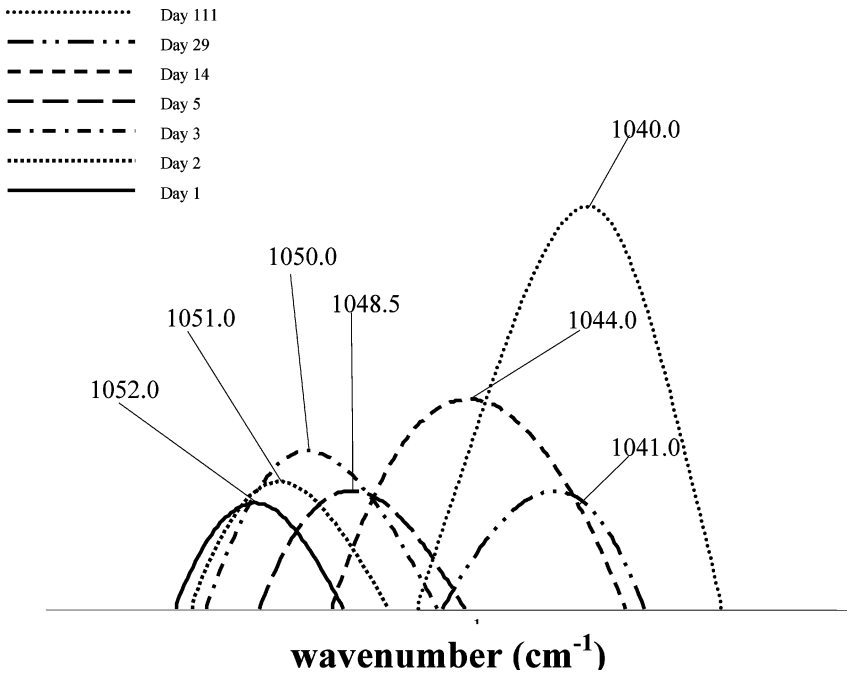

Figure 8. Expanded IR region of the symmetric sulfonate peak showing the shifting to lower wavenumbers with increasing exposure to a water-saturated environment.

curve. This dry and shifted wet data matches the hard-sphere relationship developed by De Kruif et al.[12]

$$\frac{\mu_o}{\eta} = \left(1 - \frac{\phi_{HS}}{0.63}\right)^{-2} \quad (5)$$

where μ_o is the dispersion low shear viscosity and η is the solvent viscosity. This is the solid line shown in Figure 12. This is very strong evidence that the OBSA particles remain hard sphere in nature even with the addition of water.

(12) De Kruif, C. G., et al. *J. Chem. Phys.* **1985**, *83*, 4717−4725.

Table 1. Scattering Length Densities Used for Core and Core−Shell Fits

material	mass density/ g cm^{-3}	ρ_{coh} / 10^{10} cm^{-2}
calcium carbonate	2.0	3.47
calcium carbonate	2.2	3.90
calcium carbonate	2.4	4.25
calcium carbonate	2.6	4.61
calcium carbonate	2.8	4.96
cyclohexane	0.78	−0.28
D-cyclohexane	0.8	6.72
D_2O	1.1	6.38

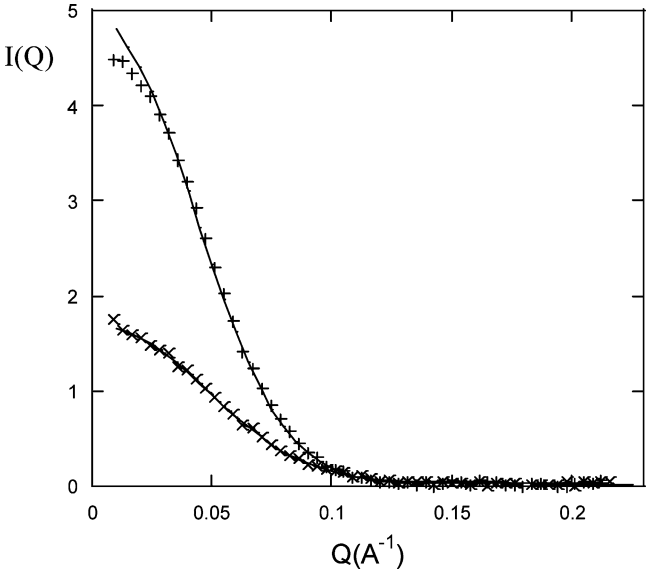

Figure 9. Data from the undoped (×) and D_2O-doped (+) OBSA cyclohexane dilutions fitted to a core radius of 2.79 nm and to the same radius with a surrounding shell of 0.44-nm-thick D_2O. The density of the calcium carbonate core was set at 2 g cm^{-3}. In both profiles, every other data point has been removed to show the fit more clearly.

Table 2. Parameter Values Used in Fitting to a Shell of D_2O around the Calcium Cores of the OBSA Particles

$CaCO_3$ density/ g cm^{-3}	polydispersity	ϕ_p	R_{HS}/ nm	R_A/ nm	R_C/ nm	fit variance/ cm^{-2}
2.0	0.2	0.0087	5.61	0.44	2.79	4.7
2.2	0.2	0.0070	5.61	0.45	2.79	5.2
2.4	0.2	0.0060	5.61	0.46	2.79	5.8
2.6	0.2	0.0051	5.61	0.46	2.79	6.4
2.8	0.2	0.0045	5.61	0.48	2.79	7.0

Table 3. Parameters and Fitted Values Used and Obtained in the Surfactant Layer Length Fits

$CaCO_3$ density/ g cm^{-3}	polydispersity	ϕ_p	R_{HS}/ nm	R_A/ nm	R_C/ nm	fit variance/ cm^{-2}
2.0	0.2	0.0072	5.61	1.42	2.79	356
2.2	0.2	0.0058	5.61	1.62	2.79	152
2.4	0.2	0.0050	5.61	1.76	2.79	143
2.6	0.2	0.0042	5.61	1.91	2.79	234
2.8	0.2	0.0037	5.61	2.02	2.79	368

Initial radius values ranging from 4.2 to 5.6 nm were experimented with, and an increase in the range of 0.05 to 0.06 nm was found to be adequate to collapse the data for the resultant range of volume fractions. Although not presented here, the viscosities of water-doped dodecane solutions of sulfonate surfactant were also measured at various volume fractions. The viscosity of the wet samples was reduced in comparison to their dry analogues, proving that the increase in viscosity observed in the OBSA dilutions does not originate from free surfactant.

Discussion

The FTIR study demonstrates the existence of water−sulfonate interactions through shifts in the sulfonate peaks. The shifting to lower wave numbers of the symmetric sulfonate peak has been explained through H-bonding between water and the sulfonate group, a weakening of the cationic−anionic interaction on hydration, and an increase in the spatial separation of adjacent sulfonate groups on hydration caused by an associated increase

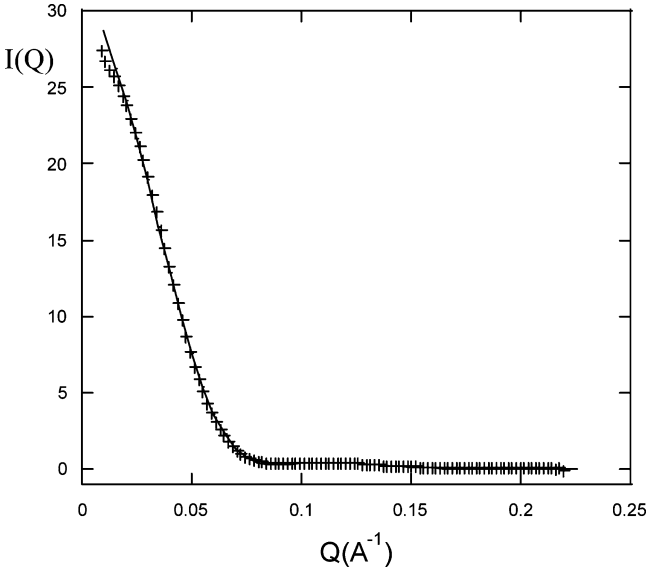

Figure 10. Scattering produced from an OBSA dilution in D-cyclohexane superimposed with a fit calculated by assuming that the calcium carbonate density is 2.4 g cm^{-3}. The calculated surfactant layer length was 1.76 nm.

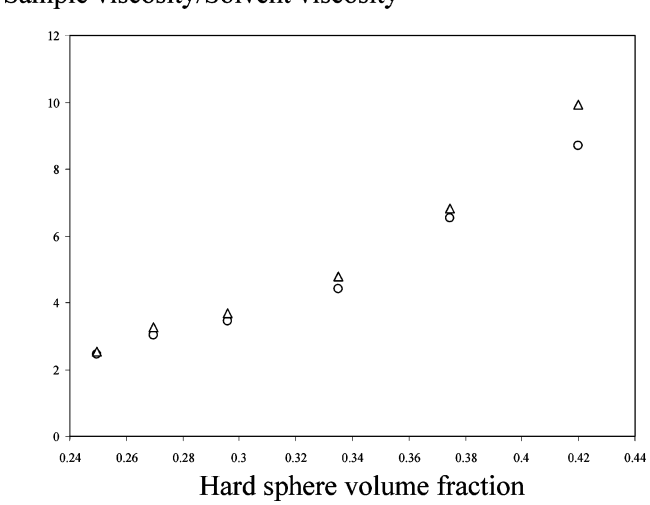

Figure 11. Comparison of the viscosity results of dry (○) and wet (Δ) samples with various volume fractions.

in cation−sulfonate separation.[13,14] The shifting in the asymmetric doublet also signifies H-bonding and reinforces the existence of water−sulfonate interactions. Broadening of the sulfonate IR peaks is also evidence of a phenomenom that has previously been attributed to H-bonding interactions with calcium sulfonates.[15] It is difficult to know if the water band at around 3200 cm^{-1} is a result of type 2 attachment water, water in the second hydration layer, or the scissor vibration of the water molecule but is further confirmation that water is hydrating the cation−anion is given by the position of the water peak at 1639 cm^{-1}, which is in agreement with previous hydration measurements of calcium ions[15] because "free" water displays an IR peak at 1595 cm^{-1}.[15] The larger and broader water peak at around 3400 cm^{-1} is likely to be water that is interacting with the cation through its oxygen while simultaneously H-bonding to the overlying

(13) Moran, P. D., et al. *J. Mater. Chem.* **1995**, *5*, 295−302.
(14) Moran, P. D.; Bowmaker, G. A.; Cooney, R. P.; Bartlett, J. R.; Woolfrey, J. L. *Langmuir* **1995**, *11*, 738−743.
(15) Zundel, G. *Hydration and Intermolecular Interaction; Infrared Investigations with Polyelectrolyte Membranes*. 1969: Academic Press, Inc.

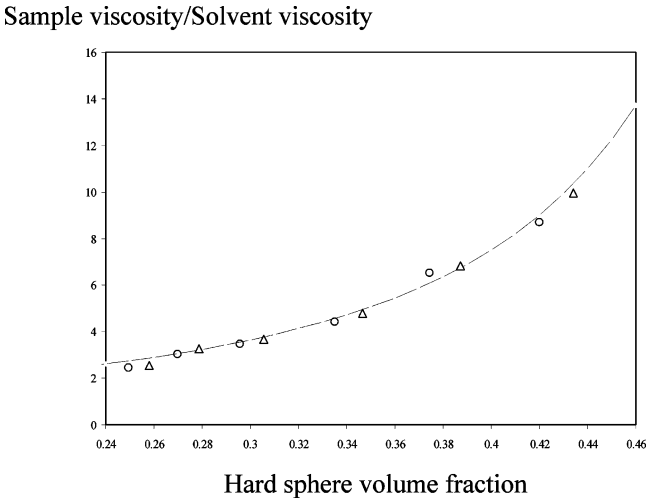

Figure 12. Shifted wet (Δ) and nonshifted dry (○) viscosity results. The shift in the wet volume fraction is a result of an increased radius of 0.05 nm/particle. The dashed line represents the de Kruif hard-sphere relationship with no fitting parameters.

sulfonate groups. If a further hydration layer is established, then this water (now type 1 water) H-bonds to the oxygens of these overlaying water molecules. Previous studies[13,14,16,17] have demonstrated that a proportion of water molecules interacting with a sulfonate group and its counterion are non-freezable. The degree of band splitting in the asymmetric sulfonate doublet also varies with water uptake. Such splitting is a facet of the antisymmetric environment in which the three S−O bonds interact with the calcium ion,[15] and increased splitting signifies increased cation−anion interaction whereas decreased splitting signifies the opposite. In Figure 7, one can see that initially splitting is increased, but after day 5, splitting begins to decrease. The decrease in splitting can be easily explained by an increase in separation between the cation and anion as hydration layers build up between the two as well as a disruption of the polarization of the anion by the cation due to the presence of water. However, the initial decrease is harder to explain though it indicates that water initially does not settle between the cation and the anion.

The SANS experiments provide compelling evidence for the formation of a shell of D_2O around the calcium carbonate core some 0.44−0.48 nm thick. Through the FTIR work, one can stipulate that such a formation is stabilized through water interactions with the sulfonate−calcium ions present on the surface. Of course, it would be natural for water to migrate to the calcium carbonate/calcium hydroxide surface even in the absence of such interactions because it provides a hydrophilic site for the water to settle.

The increase in effective volume fraction observed in the rheometry work is explained by the water-induced increase in the calcium ion−sulfonate group separation having the knock-on effect of minimally increasing the length of the surfactant layer.

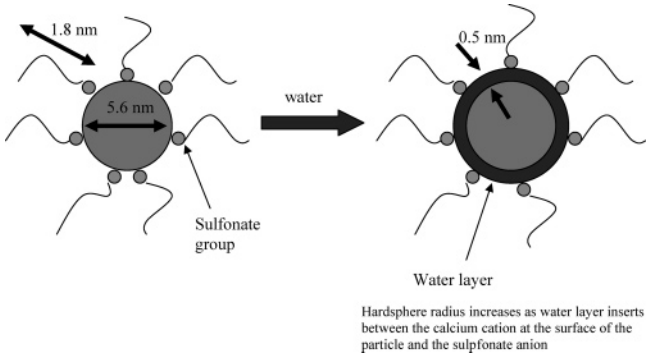

Figure 13. Proposed model for the location of water on OBSA particles.

The collapse of all viscometry data to the de Kruif correlation for hard spheres indicates that there are minimal repulsive interactions operating in the system. Although a 0.5 nm layer of water corresponds to only a few water molecules, it is possible to imagine a separation of ions and the corresponding electrostatic repulsion between particles. This is not observed in these experiments.

The DLS results demonstrate that apolar OBSA dilutions are stable with respect to water, and this is consistent with the proposed water shell model because steric stabilization would be maintained. The diameter obtained from light scattering of approximately 12 nm is in reasonable accordance with SANS results where the sum of the core and surfactant layer length is (at 2.4 g cm^{-3}) ∼4.5 nm, hence giving a diameter of 9 nm. The disparity is likely to arise from errors in the sample viscosity in the DLS measurements because some base oil will also be present. A schematic of the proposed model is shown in Figure 13.

Conclusions

We have amassed compelling evidence that water forms a layer around the core of OBSA particles on its addition to OBSA cylohexane/dodecane solutions. Rheology and light scattering results indicate that the particles remain sterically stabilized and noninteracting. FTIR results indicate an interaction between water and the sulfonate anion. SANS results prove the presence of water on the particle surface with a film thickness of 0.4 to 0.6 nm. Such an observation is significant because it represents a quantitative characterization of effectively a monolayer of water molecules using small-angle neutron scattering. Through the use of OBSA particles, the variation in neutron scattering length density can be achieved between the calcium carbonate (core), the hydrocarbon solvent/surfactant (shell), and the deuterated water layer. This has provided a quantification of results to much finer resolution than can usually be applied.

Acknowledgment. We gratefully acknowledge Peter Styring and Richard Heenan for helpful discussions and financial support from Infineum UK and EPSRC.

LA703680E

(16) Hauser, H., et al. *Interaction of water with sodium bis(2-ethyl-1-hexyl) sulfosuccinate in reversed micelles.* **1989**, *93,* 7869−7876.

(17) Wong, J.; Thomas, K.; Nowak, T. *J. Am. Chem. Soc.* **1981**, *85*, 4730−4736.